Reprinted from

CMES

Computer Modeling in Engineering & Sciences

Founder and Editor-in-Chief:
Satya N. Atluri
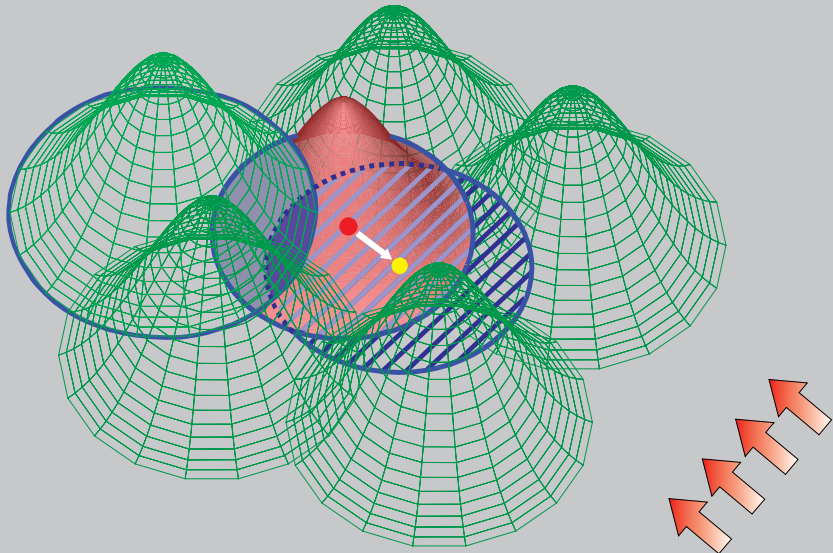
Tech Science Press

Concurrent Atomistic/Continuum Simulation of Thermo-Mechanical Coupling Phenomena

Xianqiao Wang[1] **and James D. Lee**[1]

Abstract: The concurrent methods for coupling molecular dynamics with continuum thermodynamics offer a myriad of challenging problems, mostly related with energy transmission, wave reflection, and damage propagation at the interfaces between the continuum description and the discrete description. In this work, by virtue of the atomistic field theory (AFT), we present an analysis to reconcile the compatibility between atomic region and continuum region and to calculate the matching temperature field of a heat conduction problem in a concurrent atomistic/continuum system. First, formulation of AFT with finite temperature and its corresponding finite element implementation are briefly introduced. Then we develop a new explicit algorithm with multiple-time-scale procedure to treat interfaces between atomic and continuum regions. Finally, AFT with this special algorithm is employed to investigate a thermal-mechanical coupling problem. This work provides a more fundamental understanding of thermomechanical phenomena at the interface between atomic and continuum regions.

Keywords: Molecular dynamics; Thermomechanical coupling; Multiscale modeling; Heat conduction; Temperature; Atomistic field theory

1   Introduction

It is understood that continuum physics is invalid for material systems at nanoscale; and, even with a state-of-the-art supercomputer, molecular dynamics (MD) simulation is limited in the length/time scale that it can handle. Yet, ultimately we aim at the design and manufacture of synthetic and hierarchical material systems or structures in which the organization is designed and controlled on length scales ranging from nanoscopic to microscopic, even to macroscopic. Therefore multiscale modeling, from atom to continuum, is inevitably needed.

---

[1] George Washington University, Washington, DC 20052.   xqwang@gwmail.gwu.edu, jdlee@gwu.edu

Recently, several multiscale techniques have been developed; we will briefly review some of these works. To begin with, the coupling of length scale method (CLSM) was a pioneering work developed by Abraham, Broughton, Broughton, Bernstein, and Kaxiras (1998), and by Rudd and Broughton (2001), which incorporated the coupling of a tight-binding quantum mechanics approximation, MD, and finite element (FE) continuum model. Belytschko and Xiao (2003), Xiao and Belytschko (2004) developed the Bridging-domain method (BDM), in which the continuum and molecular domains were overlapped in a bridging subdomain, and the Hamiltonian was taken to be linear combination of the continuum and molecular parts. The compatibility in BDM was enforced by Lagrange multipliers or by the augmented Lagrangian method. The groundwork of the bridging scale method (BSM) was presented by Wagner and Liu (2003), in which the molecular displacements were decomposed into fine and coarse scales throughout the domain. At the interface between the two domains, they used a form of the Langevin equation to eliminate spurious reflections. They reported excellent results for one-dimensional problems. Also Kadowaki and Liu (2005) presented a multiscale approach for the micropolar continuum model, in which averaging procedures are operated over a surrounding sub-domain for each material point to bridge a discrete microstructure to a macro continuum model. The atomistic-to-continuum (AtC) method, developed by Fish, Nuggehally, Shephard, Picu, Badia, Parks and Gunzburger (2007), and by Parks, Bochev and Lehoucq (2008), was a force-based method which achieved the coupling between atomistic and continuum region by blending at the level of forces. In these fashions, the computational power is harnessed, resulting in an optimum compromise between numerical accuracy and computational overhead. The multiscale simulation technique based on the meshless local Petrov-Galerkin method was developed by Shen and Atluri (2004 a, b, c), in which several alternate time-dependent interfacial conditions, between the atomistic and continuum regions, are systematically studied, for the seamless multiscale simulation, by decomposing the displacement of atoms in the equivalent continuum region into long and short wave-length components. Ma et al. (2006) also developed a multiscale simulation method using generalized interpolation material point method (GIMP) and molecular dynamics. In their theory, a material point in the continuum is split into smaller material points using multi-level refinement until it has nearly reached the atom size to couple with atoms in the MD region. Consequently, coupling between GIMP and MD is achieved by using compatible deformation, force, and energy fields in the transition region between GIMP and MD. Raghavan and Ghosh (2004) established an adaptive multiscale computational modeling of composite materials that combines a conventional displacement based finite element model with a microstructural Voronoi cell finite element model for multi-scale analysis of composite structures with non-uniform microstructural heterogeneities as obtained from

optical or scanning electron micrographs. Compared with direct atomistic simulation, these techniques have the potential to produce significant time and length scale gains by treating smoothly varying regions of the configurational space collectively. Generally speaking, however, in all those above-mentioned coupled methods, the idea is to use a fully atomistic description in one region of material and a continuum description in other regions. The detailed treatment of the material in the 'transition region' or boundary between the atomistic and continuum regions is a critical aspect of such an approach.

The Quasicontinuum (QC) method, developed by Tadmor, Ortiz and Phillips (1998) and extended by Knap and Ortiz (2001), has been used to study a variety of fundamental aspects of deformation in crystalline solids at zero temperature based on Cauchy-Born elasticity. In most works based on QC method, triangular finite elements or tetrahedral finite elements for continuum region is adopted in 2D or 3D simulation, thereby leading to a locally-uniform deformation gradient in the continuum region. Linear interpolation functions in triangular or tetrahedral finite element require only one single Gauss-point for numerical quadrature. As a consequence, the application of the Cauchy-Born rule (CBR) implies that in the energy calculation the summation over the number of lattice sites boils down to the number of finite elements. Therefore, there will be a limitation for QC methods due to the validity of the kinematic assumption of CBR, i.e., to determine the state when a transition to non-affine deformations is possible due to instabilities or inhomogeneous of the underlying atomic system (Stienmann, Elizondo and Sunyk, 2006). Later, several versions of finite-temperature extension of QC method are obtained: (1) by presenting a derivation of an effective energy function to perform Monte Carlo simulation in concurrent atomistic continuum setting (Shenoy, Shenoy and Phillips, 1999); (2) by employing the temperature-related Cauchy-Born rule with free energy instead of potential energy (Xiao and Yang, 2007); (3) by using dissipative Langevin dynamics (Marian, Venturini, Hansen, Knap, Ortiz and Campbell, 2010). However, in these procedures the energy equation was based on the classical heat conduction assumption including Fourier's law, which may be questionable in micro/nano system. It is worthwhile to mention that in its original version the QC method was formulated for simple crystals with one atom per unit cell (Simth, Tadmor, Bernstein and Kaxiras, 2001). However, one has to mention that Tadmor, Smith, Bernstein, and Kaxiras (1999) extended the QC method to simulate materials with multiple atoms in a unit cell. It should also be emphasized that the Cauchy-Born rule certainly is not appropriate to materials with multiple atoms in a unit cell.

To circumvent the difficulties mentioned above, an atomistic field theory has been constructed by Chen and her co-workers (Chen and Lee, 2005; Chen, 2006 and

2009) for concurrent atomistic/continuum modeling of materials systems. In this work, we develop an approach to reconcile the compatibility between atomic region and continuum region and to calculate the temperature field of a thermo-mechanical coupling problem. To enhance the computational efficiency, we introduce and utilize a multiple-time-scale algorithm. The organization of the remainder of the paper is as follows: In Section 2, we briefly present the atomistic field theory. By means of virtual work, in Section 3 we provide the finite element formulation of AFT. Section 4 contains the numerical procedure to deal with the interface between atomic region and continuum region in AFT simulation. Finally we show the numerical results of a sample problem and conclude this paper with a brief summary and discussion in Section 5 and Section 6, respectively.

2 Atomistic Field Theory

To provide the background for subsequent developments, we briefly review the atomistic field theory developed by Chen and her co-workers. AFT views a crystalline material as a continuous collection of lattice cells, while situated within each lattice cell is a group of discrete atoms as shown in Fig. 1. From this viewpoint, we recall a general link, rigorously developed by Chen (2009), between any phase space function $\mathbf{A}(\mathbf{r}, \mathbf{p})$ and its corresponding local density function $\mathbf{a}(\mathbf{x}, \mathbf{y}^\alpha, t)$ as follows

$$\mathbf{a}(\mathbf{x}, \mathbf{y}^\alpha, t) = \sum_{k=1}^{N_l} \sum_{\xi=1}^{N_a} \mathbf{A}(\mathbf{r}, \mathbf{p}) \delta[\mathbf{R}^k(t) - \mathbf{x}] \tilde{\delta}[\Delta \mathbf{r}^{k\xi}(t) - \mathbf{y}^\alpha] \quad (\alpha = 1, 2, 3, \cdots, N_a) \quad (1)$$
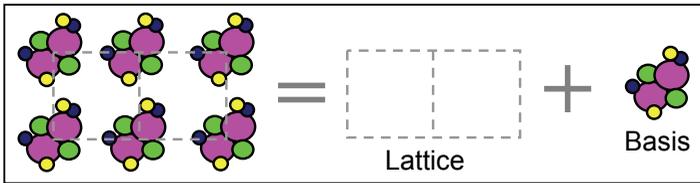

Figure 1: Atomistic view of crystal structure

with

$$\mathbf{r} \equiv \{ \mathbf{R}^{k\alpha} = \mathbf{R}^k + \Delta \mathbf{r}^{k\alpha} \, | \, k = 1, 2, 3, ..., N_l \, , \, \alpha = 1, 2, 3, ..., N_a \}$$
$$\mathbf{p} \equiv \{ m^\alpha \mathbf{V}^{k\alpha} = m^\alpha (\mathbf{V}^k + \Delta \mathbf{v}^{k\alpha}) \, | \, k = 1, 2, 3, ..., N_l \, , \, \alpha = 1, 2, 3, ..., N_a \} \quad (2)$$

$$\int_V \delta(\mathbf{R}^k - \mathbf{x})d\mathbf{x} = 1$$

$$\tilde{\delta}(\Delta\mathbf{r}^{k\xi} - \mathbf{y}^\alpha) = \int_{V(\mathbf{y}^\alpha)} \delta(\Delta\mathbf{r}^{k\xi} - \mathbf{y})d\mathbf{y} = \begin{cases} 1 & \text{if } \xi = \alpha \text{ and } \Delta\mathbf{r}^{k\alpha} = \mathbf{y}^\alpha \\ 0 & \text{otherwise} \end{cases} \tag{3}$$

Here the superscript $k\xi$ refers to the ξth atom in the kth unit cell; $\mathbf{R}^k$ is the position of the mass center of the kth unit cell; $\Delta\mathbf{r}^{k\xi}$ is the atomic position of the ξth atom relative to the mass center of the kth unit cell; N_l is the total number of unit cells in the system; N_a is the number of atoms in a unit cell; V is the volume of the whole system; $V(\mathbf{y}^\alpha)$ is the volume of αth atom in the unit cell. The first delta function in eq. (1) is a localization function. It can be a Dirac δ-function, or a distribution function as suggested by Hardy (1982). However, it should be noted that the field descriptions of the conservation equations and the constitutive relations have been proved to be independent of the choices of the localization function. The second delta function in eq. (1) is the Kronecker delta, which identifies $\mathbf{y}^\alpha$ to $\Delta\mathbf{r}^{k\alpha}$.

The time evolution of any physical quantity in the atomistic field theory can be expressed as:

$$\begin{aligned}
\frac{\partial \mathbf{a}(\mathbf{x}, \mathbf{y}^\alpha, t)}{\partial t}\bigg|_{\mathbf{x},\mathbf{y}^\alpha} &= \sum_{k=1}^{N_l}\sum_{\xi=1}^{N_a} \dot{\mathbf{A}}(\mathbf{r},\mathbf{p})\delta(\mathbf{R}^k - \mathbf{x})\tilde{\delta}(\Delta\mathbf{r}^{k\xi} - \mathbf{y}^\alpha) \\
&\quad - \nabla_\mathbf{x} \cdot \sum_{k=1}^{N_l}\sum_{\xi=1}^{N_a} \mathbf{V}^k \otimes \mathbf{A}(\mathbf{r},\mathbf{p})\delta(\mathbf{R}^k - \mathbf{x})\tilde{\delta}(\Delta\mathbf{r}^{k\xi} - \mathbf{y}^\alpha) \\
&\quad - \nabla_{\mathbf{y}^\alpha} \cdot \sum_{k=1}^{N_l}\sum_{\xi=1}^{N_a} \Delta\mathbf{v}^{k\xi} \otimes \mathbf{A}(\mathbf{r},\mathbf{p})\delta(\mathbf{R}^k - \mathbf{x})\tilde{\delta}(\Delta\mathbf{r}^{k\xi} - \mathbf{y}^\alpha)
\end{aligned} \tag{4}$$

When $\mathbf{a}(\mathbf{x}, \mathbf{y}^\alpha, t)$ is the local density of a conserved quantity, eq. (4) represents the corresponding balance law.

By virtue of eq. (1), the local density quantities, such as mass density ρ^α, linear momentum density $\rho^\alpha(\mathbf{v} + \Delta\mathbf{v}^\alpha)$, interatomic force density $\mathbf{f}^\alpha$, external force density ϕ^α, the homogeneous part t^α and inhomogeneous part τ^α of stress tensor, internal energy density $\rho^\alpha e^\alpha$, the homogeneous part $\mathbf{q}^\alpha$ and inhomogeneous part $\mathbf{j}^\alpha$ of heat flux, heat source h^α, and temperature T^α, are defined as

$$\rho^\alpha \equiv \sum_{k=1}^{N_l}\sum_{\xi=1}^{N_a} m^\xi \delta(\mathbf{R}^k - \mathbf{x})\tilde{\delta}(\Delta\mathbf{r}^{k\xi} - \mathbf{y}^\alpha) \tag{5}$$

$$\rho^\alpha(\mathbf{v} + \Delta\mathbf{v}^\alpha) \equiv \sum_{k=1}^{N_l}\sum_{\xi=1}^{N_a} m^\xi(\mathbf{V}^k + \Delta\mathbf{v}^{k\xi})\delta(\mathbf{R}^k - \mathbf{x})\tilde{\delta}(\Delta\mathbf{r}^{k\xi} - \mathbf{y}^\alpha) \tag{6}$$

$$\mathbf{f}^{\alpha} \equiv \sum_{k=1}^{N_l} \sum_{\xi=1}^{N_a} (-\partial U / \partial \mathbf{R}^{k\xi}) \delta(\mathbf{R}^k - \mathbf{x}) \tilde{\delta}(\Delta \mathbf{r}^{k\xi} - \mathbf{y}^{\alpha})$$

$$= \sum_{k=1}^{N_l} \sum_{\xi=1}^{N_a} \mathbf{F}^{k\xi} \delta(\mathbf{R}^k - \mathbf{x}) \tilde{\delta}(\Delta \mathbf{r}^{k\xi} - \mathbf{y}^{\alpha}) \tag{7}$$

$$\boldsymbol{\varphi}^{\alpha} \equiv \sum_{k=1}^{N_l} \sum_{\xi=1}^{N_a} \mathbf{F}_{ext}^{k\xi} \delta(\mathbf{R}^k - \mathbf{x}) \tilde{\delta}(\Delta \mathbf{r}^{k\xi} - \mathbf{y}^{\alpha}) \tag{8}$$

$$\mathbf{t}^{\alpha} = \mathbf{t}_{kin}^{\alpha} + \mathbf{t}_{pot}^{\alpha}$$

$$\equiv - \sum_{k=1}^{N_l} \sum_{\xi=1}^{N_a} m^{\xi} \tilde{\mathbf{V}}^k \otimes \tilde{\mathbf{V}}^{k\xi} \delta(\mathbf{R}^k - \mathbf{x}) \tilde{\delta}(\Delta \mathbf{r}^{k\xi} - \mathbf{y}^{\alpha})$$

$$- \frac{1}{2} \sum_{k,l=1}^{N_l} \sum_{\xi,\eta=1}^{N_a} (\mathbf{R}^k - \mathbf{R}^l) \otimes \mathbf{F}^{k\xi} B(k,\xi,l,\eta,\mathbf{x},\mathbf{y}^{\alpha}) \tag{9}$$

$$\boldsymbol{\tau}^{\alpha} = \boldsymbol{\tau}_{kin}^{\alpha} + \boldsymbol{\tau}_{pot}^{\alpha}$$

$$\equiv - \sum_{k=1}^{N_l} \sum_{\xi=1}^{N_a} m^{\xi} \Delta \tilde{\mathbf{v}}^{k\xi} \otimes \tilde{\mathbf{V}}^{k\xi} \delta(\mathbf{R}^k - \mathbf{x}) \tilde{\delta}(\Delta \mathbf{r}^{k\xi} - \mathbf{y}^{\alpha})$$

$$- \frac{1}{2} \sum_{k,l=1}^{N_l} \sum_{\xi,\eta=1}^{N_a} (\Delta \mathbf{r}^{k\xi} - \Delta \mathbf{r}^{l\eta}) \otimes \mathbf{F}^{k\xi} B(k,\xi,l,\eta,\mathbf{x},\mathbf{y}^{\alpha}) \tag{10}$$

$$\rho^{\alpha} e^{\alpha} \equiv \sum_{k=1}^{N_l} \sum_{\xi=1}^{N_a} [\tfrac{1}{2} m^{\xi} (\tilde{\mathbf{V}}^{k\xi})^2 + U^{k\xi}] \delta(\mathbf{R}^k - \mathbf{x}) \tilde{\delta}(\Delta \mathbf{r}^{k\xi} - \mathbf{y}^{\alpha}) \tag{11}$$

$$\mathbf{q}^{\alpha} = \mathbf{q}_{kin}^{\alpha} + \mathbf{q}_{pot}^{\alpha}$$

$$\equiv - \sum_{k=1}^{N_l} \sum_{\xi=1}^{N_a} \tilde{\mathbf{V}}^k \left(\tfrac{1}{2} m^{\xi} (\tilde{\mathbf{V}}^{k\xi})^2 + U^{k\xi} \right) \delta(\mathbf{R}^k - \mathbf{x}) \tilde{\delta}(\Delta \mathbf{r}^{k\xi} - \mathbf{y}^{\alpha})$$

$$- \frac{1}{2} \sum_{k,l=1}^{N_l} \sum_{\xi,\eta=1}^{N_a} (\mathbf{R}^k - \mathbf{R}^l) \tilde{\mathbf{V}}^{k\xi} \cdot \mathbf{F}^{k\xi} B(k,\xi,l,\eta,\mathbf{x},\mathbf{y}^{\alpha}) \tag{12}$$

$$\mathbf{j}^{\alpha} = \mathbf{j}_{kin}^{\alpha} + \mathbf{j}_{pot}^{\alpha}$$

$$\equiv - \sum_{k=1}^{N_l} \sum_{\xi=1}^{N_a} \Delta \tilde{\mathbf{v}}^{k\xi} \left(\tfrac{1}{2} m^{\xi} (\tilde{\mathbf{V}}^{k\xi})^2 + U^{k\xi} \right) \delta(\mathbf{R}^k - \mathbf{x}) \tilde{\delta}(\Delta \mathbf{r}^{k\xi} - \mathbf{y}^{\alpha})$$

$$- \frac{1}{2} \sum_{k,l=1}^{N_l} \sum_{\xi,\eta=1}^{N_a} (\Delta \mathbf{r}^{k\xi} - \Delta \mathbf{r}^{l\eta}) \tilde{\mathbf{V}}^{k\xi} \cdot \mathbf{F}^{k\xi} B(k,\xi,l,\eta,\mathbf{x},\mathbf{y}^{\alpha}) \tag{13}$$

$$h^\alpha \equiv \sum_{k=1}^{N_l} \sum_{\xi=1}^{N_a} \tilde{\mathbf{V}}^{k\xi} \cdot \mathbf{F}_{ext}^{k\xi} \delta(\mathbf{R}^k - \mathbf{x}) \tilde{\delta}(\Delta \mathbf{r}^{k\xi} - \mathbf{y}^\alpha) \tag{14}$$

$$T^\alpha \equiv \frac{\Delta V}{3k_B} \sum_{k=1}^{N_l} \sum_{\xi=1}^{N_a} m^\xi (\tilde{\mathbf{V}}^{k\xi})^2 \delta(\mathbf{R}^k - \mathbf{x}) \tilde{\delta}(\Delta \mathbf{r}^{k\xi} - \mathbf{y}^\alpha) \tag{15}$$

where $\tilde{\mathbf{V}}^{k\xi} \equiv \mathbf{V}^{k\xi} - (\mathbf{v} + \Delta \mathbf{v}^\xi)$ is the difference between phase space velocity and local physical space velocity; $U^{k\xi}$ is the potential energy of $k\xi$th atom; $U = \sum_{k=1}^{N_l} \sum_{\xi=1}^{N_a} U^{k\xi}$ is the total potential energy; k_B is the Boltzmann constant; ΔV is the volume of unit cell, and $B(k, \xi, l, \eta, \mathbf{x}, \mathbf{y}^\alpha)$ is defined as

$$B(k, \xi, l, \eta, \mathbf{x}, \mathbf{y}^\alpha) \equiv$$
$$\int_0^1 \delta\left(\mathbf{R}^k \lambda + \mathbf{R}^l (1-\lambda) - \mathbf{x}\right) \tilde{\delta}\left(\Delta \mathbf{r}^{k\xi} \lambda + \Delta \mathbf{r}^{l\eta} (1-\lambda) - \mathbf{y}^\alpha\right) d\lambda \tag{16}$$

Following eq. (4), as exact consequences of Newton's second laws, we have the time evolution of conserved quantities, namely, mass, linear and angular momenta, and energy, as (Chen and Lee, 2005; Chen, 2006 and 2009):

$$\frac{d\rho^\alpha}{dt} + \rho^\alpha \nabla_{\mathbf{x}} \cdot \mathbf{v} + \rho^\alpha \nabla_{\mathbf{y}^\alpha} \cdot \Delta \mathbf{v}^\alpha = 0 \tag{17}$$

$$\rho^\alpha \frac{d}{dt}(\mathbf{v} + \Delta \mathbf{v}^\alpha) = \nabla_{\mathbf{x}} \cdot \mathbf{t}^\alpha + \nabla_{\mathbf{y}^\alpha} \cdot \boldsymbol{\tau}^\alpha + \varphi^\alpha \tag{18}$$

$$\mathbf{t}^\alpha + \boldsymbol{\tau}^\alpha = (\mathbf{t}^\alpha + \boldsymbol{\tau}^\alpha)^T \tag{19}$$

$$\rho^\alpha \frac{de^\alpha}{dt} + \nabla_{\mathbf{x}} \cdot (-\mathbf{q}^\alpha) + \nabla_{\mathbf{y}^\alpha} \cdot (-\mathbf{j}^\alpha) = \mathbf{t}^\alpha : \nabla_{\mathbf{x}}(\mathbf{v} + \Delta \mathbf{v}^\alpha) + \boldsymbol{\tau}^\alpha : \nabla_{\mathbf{y}^\alpha}(\mathbf{v} + \Delta \mathbf{v}^\alpha) + h^\alpha \tag{20}$$

It is worthwhile to note that, with the atomistic definitions of interatomic force and the potential parts of the atomic stresses, one has (Chen and Lee, 2005)

$$\nabla_{\mathbf{x}} \cdot \mathbf{t}_{pot}^\alpha + \nabla_{\mathbf{y}^\alpha} \cdot \boldsymbol{\tau}_{pot}^\alpha = \mathbf{f}^\alpha \tag{21}$$

For a single-element atomic system, Cheung and Yip (1991) and Haile (2001) gave the following definitions for kinetic stresses $\hat{t}_{ij}$ and temperature $\hat{T}$:

$$\hat{t}_{ij} = -\sum_{l=1}^{N} m\tilde{v}_i^l \tilde{v}_j^l / \hat{V}, \quad 3Nk_B\hat{T} = \sum_{l=1}^{N} m\tilde{v}_i^l \tilde{v}_i^l \tag{22}$$

where $\hat{V}$ is the volume that the atoms occupy; $\tilde{v}_i^l$ is the difference velocity of the ith component between instantaneous velocity and average velocity of the lth atom. In consistent with Cheung and Yip (1991) and Haile (2001), for multi-element atomic system, we have

$$
\begin{aligned}
\mathbf{t}_{kin}^{\alpha} &= -m^{\alpha}\tilde{\mathbf{v}} \otimes (\tilde{\mathbf{v}} + \Delta\tilde{\mathbf{v}}^{\alpha})/\Delta V \\
\boldsymbol{\tau}_{kin}^{\alpha} &= -m^{\alpha}\Delta\tilde{\mathbf{v}}^{\alpha} \otimes (\tilde{\mathbf{v}} + \Delta\tilde{\mathbf{v}}^{\alpha})/\Delta V \\
3k_B T^{\alpha} &= m^{\alpha}(\tilde{\mathbf{v}} + \Delta\tilde{\mathbf{v}}^{\alpha}) \cdot (\tilde{\mathbf{v}} + \Delta\tilde{\mathbf{v}}^{\alpha})
\end{aligned}
\tag{23}
$$

It is seen that $\mathbf{t}_{kin}^{\alpha} + \boldsymbol{\tau}_{kin}^{\alpha} = -m^{\alpha}(\tilde{\mathbf{v}} + \Delta\tilde{\mathbf{v}}^{\alpha}) \otimes (\tilde{\mathbf{v}} + \Delta\tilde{\mathbf{v}}^{\alpha})/\Delta V$ is symmetric; but neither $\mathbf{t}_{kin}^{\alpha}$ nor τ_{kin}^{α} is symmetric. At temperature higher than Debye temperature and within harmonic approximation, all modes have the same energy (Dove, 1993). This implies

$$
(N_a - 1)m\tilde{\mathbf{v}} \cdot \tilde{\mathbf{v}} = \sum_{\alpha=1}^{N_a} m^{\alpha}\Delta\tilde{\mathbf{v}}^{\alpha} \cdot \Delta\tilde{\mathbf{v}}^{\alpha}
\tag{24}
$$

where $m = \sum_{\alpha=1}^{N_a} m^{\alpha}$ is the total mass of a unit cell. Equation (23) implies

$$
t_{ij(kin)}^{\alpha} = -\frac{\lambda^{\alpha}k_B T \delta_{ij}}{\Delta V}, \qquad \tau_{ij(kin)}^{\alpha} = -\frac{(1 - \lambda^{\alpha})k_B T \delta_{ij}}{\Delta V}
\tag{25}
$$

where $\lambda^{\alpha} = m^{\alpha}/m$. Definition of temperature at nanoscale is still a debating issue. Here, we follow the classical way to define temperature as a measure of thermal energy over a finite duration and over a unit cell. Thus, we have $T^{\alpha} = T(\mathbf{x}, t)$ and $\nabla_{\mathbf{y}^{\alpha}} \cdot \boldsymbol{\tau}_{kin}^{\alpha} = 0$. Now the governing equation, eq. (18), can be rewritten as

$$
\rho^{\alpha}\ddot{\mathbf{u}}^{\alpha}(\mathbf{x}, t) = -\frac{\gamma^{\alpha}k_B \nabla T(\mathbf{x}, t)}{\Delta V} + \mathbf{f}^{\alpha}(\mathbf{x}, t) + \boldsymbol{\varphi}^{\alpha}(\mathbf{x}, t)
\tag{26}
$$

where $\dot{\mathbf{u}}^{\alpha}(\mathbf{x}, t) = \mathbf{v} + \Delta\mathbf{v}^{\alpha}$, $\ddot{\mathbf{u}}^{\alpha}(\mathbf{x}, t) = \frac{d(\mathbf{v} + \Delta\mathbf{v}^{\alpha})}{dt}$.

In lattice systems, the smallest allowable physical volume in AFT is the volume of a unit cell. The mass density of the αth atom at $\mathbf{x}$ is thus $\rho^{\alpha}(\mathbf{x}, t) = m^{\alpha}/\Delta V(\mathbf{x}, t)$, where m^{α} is the mass of the αth atom. Consider the specimen as a material system made of two regions: continuum region (N_l unit cells) and atomic region (N atoms), as shown in Fig. 2 (here a 2D picture is shown for the purpose of illustration). Each unit cell has N_a atoms. Then the governing equation in these two regions can be expressed as

Continuum region $[\alpha = 1, 2, 3, \cdots, N_a]$

$$
m^{\alpha}\ddot{\mathbf{u}}^{\alpha}(\mathbf{x}, t) = -\gamma^{\alpha}k_B \nabla T(\mathbf{x}, t) + \mathbf{F}_C^{\alpha}(\mathbf{x}, t) + \boldsymbol{\Phi}_C^{\alpha}(\mathbf{x}, t)
\tag{27}
$$
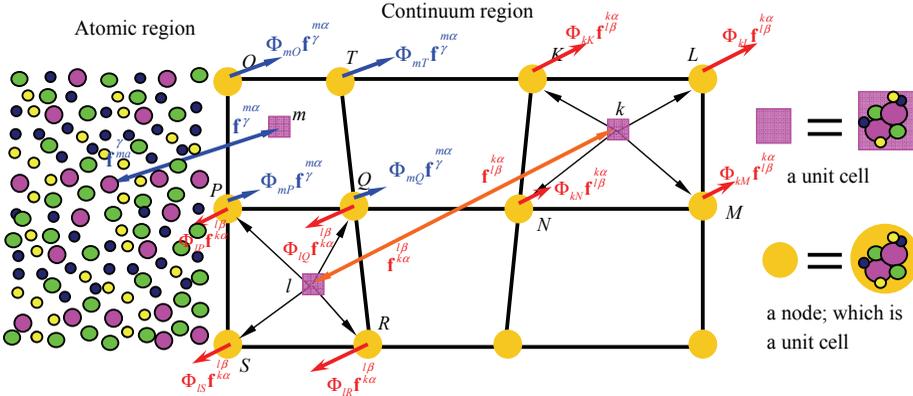
Figure 2: Schematic picture of AFT model with force distribution

where $\mathbf{F}_C^\alpha(\mathbf{x},t)$ is the interatomic force; $\boldsymbol{\Phi}_C^\alpha(\mathbf{x},t)$ is the force due to external fields.

Atomic region $[\beta = 1,2,3,...,N]$

$$m^\beta \ddot{\mathbf{u}}^\beta(t) = \mathbf{F}_A^\beta(t) + \boldsymbol{\Phi}_A^\beta(t) \tag{28}$$

where $\mathbf{F}_A^\beta(t)$ and $\boldsymbol{\Phi}_A^\beta(t)$ are the interatomic force and external force acting on the βth atom, respectively. It is seen that, in MD simulation, temperature is not an independent variable; hence it doesn't appear in the governing equations; instead it is calculated as

$$3Nk_BT = \sum_{i=1}^N m^i(\dot{\mathbf{u}}^i - \bar{\mathbf{u}}) \cdot (\dot{\mathbf{u}}^i - \bar{\mathbf{u}}) \tag{29}$$

where $\bar{\mathbf{u}}$ is the mass-weighted velocities of a group of N atoms.

In this work, the temperature in continuum region is given as a function of space and time $T = g(\mathbf{x},t)$. Then the relevant governing equations in continuum region are just the balance law for linear momentum, i.e.,

$$m^\alpha \ddot{\mathbf{u}}^\alpha(\mathbf{x},t) = \mathbf{F}_{temp}^\alpha(\mathbf{x},t) + \mathbf{F}_C^\alpha(\mathbf{x},t) + \boldsymbol{\Phi}_C^\alpha(\mathbf{x},t) \tag{30}$$

where $\mathbf{F}_{temp}^\alpha(\mathbf{x},t) = -\gamma^\alpha k_B \nabla g(\mathbf{x},t)$ is the force due to temperature.

3 Finite Element Implementation

Define $\mathbf{F}^{\xi\eta}[\mathbf{u}^{\xi},\mathbf{u}^{\eta}]$ as the interatomic force acting on the ξth atom due to the ηth atom

$$
\begin{aligned}
\mathbf{F}^{\xi\eta}[\mathbf{u}^{\xi},\mathbf{u}^{\eta}] &= -\frac{1}{2}\left(\frac{\partial U^{\xi\eta}}{\partial \mathbf{u}^{\xi}} - \frac{\partial U^{\xi\eta}}{\partial \mathbf{u}^{\eta}}\right) \\
&= \frac{1}{2}(\mathbf{F}^{\xi\eta} - \mathbf{F}^{\eta\xi})
\end{aligned}
\tag{31}
$$

where $u^{\xi\eta}$ is the interatomic potential between the ξth atom and ηth atom.

The interatomic force $\mathbf{F}_{C}^{\alpha}(\mathbf{x},t)$ in continuum region and $\mathbf{F}_{A}^{\beta}(t)$ in atomic region can be expressed respectively as (Lee, Wang and Chen, 2009a, b)

$$
\mathbf{F}_{C}^{\alpha}(\mathbf{x},t) =
$$

$$
\int_{\Omega(\mathbf{x}',t)} \frac{1}{\Delta V(\mathbf{x}',t)} \sum_{\beta=1}^{N_a} \mathbf{F}^{\alpha\beta}[\mathbf{u}^{\alpha}(\mathbf{x},t),\mathbf{u}^{\beta}(\mathbf{x}',t)]d\Omega(\mathbf{x}',t) + \sum_{\beta=1}^{N} \mathbf{F}^{\alpha\beta}[\mathbf{u}^{\alpha}(\mathbf{x},t),\mathbf{u}^{\beta}(t)]
\tag{32}
$$

$$
\mathbf{F}_{A}^{\beta}(t) = \int_{\Omega(\mathbf{x},t)} \frac{1}{\Delta V(\mathbf{x},t)} \sum_{\alpha=1}^{N_a} \mathbf{F}^{\beta\alpha}[\mathbf{u}^{\beta}(t),\mathbf{u}^{\alpha}(\mathbf{x},t)]d\Omega(\mathbf{x},t) + \sum_{\alpha=1}^{N} \mathbf{F}^{\beta\alpha}[\mathbf{u}^{\beta}(t),\mathbf{u}^{\alpha}(t)]
\tag{33}
$$

Now the weak form, based on eqs. (28) and (30), can be expressed as

$$
\int_{\Omega} \frac{1}{\Delta V(\mathbf{x})} \sum_{\alpha=1}^{N_a} \{m^{\alpha}\ddot{\mathbf{u}}^{\alpha} - \mathbf{F}_{C}^{\alpha} - \boldsymbol{\Phi}_{C}^{\alpha} - \mathbf{F}_{temp}^{\alpha}\} \cdot \delta\mathbf{u}^{\alpha}d\Omega
$$

$$
+ \sum_{\beta=1}^{N} \{m^{\beta}\ddot{\mathbf{u}}^{\beta} - \mathbf{F}_{A}^{\beta} - \boldsymbol{\Phi}_{A}^{\beta}\} \cdot \delta\mathbf{u}^{\beta} = 0 \quad (34)
$$

The displacements and the virtual displacements are expressed as

$$
\mathbf{u}^{\alpha}(\mathbf{x}) = \Phi_{I}(\mathbf{x})\mathbf{U}_{I}^{\alpha}, \; \delta\mathbf{u}^{\alpha}(\mathbf{x}) = \Phi_{I}(\mathbf{x})\delta\mathbf{U}_{I}^{\alpha}
\tag{35}
$$

where $\Phi_{I}(\mathbf{x})$ is the shape function, and $\mathbf{U}_{I}^{\alpha}$ is the displacement of αth atom within the Ith node of the element in which $\mathbf{x}$ resides. After lengthy but straightforward derivations, finally we have

Continuum region

$$
\int_{\Omega} \frac{1}{\Delta V(\mathbf{x})} m^{\alpha} \Phi_J \Phi_I \ddot{\mathbf{U}}_I^{\alpha} d\Omega
$$

$$
-\int_{\Omega} \frac{1}{\Delta V(\mathbf{x})} \Phi_J \sum_{\beta=1}^{N_a} \int_{\Omega(\mathbf{x}')} \frac{1}{\Delta V(\mathbf{x}')} \mathbf{F}^{\alpha\beta}[\Phi_I \mathbf{U}_I^{\alpha}, \Phi_K(\mathbf{x}') \mathbf{U}_K^{\beta}] d\Omega(\mathbf{x}') d\Omega \tag{36}
$$

$$
-\int_{\Omega} \frac{1}{\Delta V(\mathbf{x})} \Phi_J \sum_{\beta=1}^{N} \mathbf{F}^{\alpha\beta}[\Phi_I \mathbf{U}_I^{\alpha}, \mathbf{u}^{\beta}] d\Omega - \int_{\Omega} \frac{1}{\Delta V(\mathbf{x})} (\mathbf{F}_{temp}^{\alpha} + \Phi_C^{\alpha}) \Phi_J d\Omega = 0
$$

Atomic region

$$
m^{\beta} \ddot{\mathbf{u}}^{\beta} - \Phi_A^{\beta} - \sum_{\alpha=1}^{N} \mathbf{F}^{\beta\alpha}[\mathbf{u}^{\beta}, \mathbf{u}^{\alpha}] - \int_{\Omega} \frac{1}{\Delta V} \sum_{\alpha=1}^{N_a} \mathbf{F}^{\beta\alpha}[\mathbf{u}^{\beta}, \Phi_I \mathbf{U}_I^{\alpha}] d\Omega = 0 \tag{37}
$$

We further reduce it to a lumped-mass system. Then, for the sake of simplicity, eqs. (36, 37) are written in the following symbolic expressions

$$
M_J^{\alpha} \ddot{\mathbf{U}}_J^{\alpha} = \Sigma_J^{\alpha}(\mathbf{U}_I^{\beta}, \mathbf{u}^{\gamma}, T_I) \quad (I \in P; \quad \beta = 1, 2, \cdots, N_a; \quad \gamma = 1, 2, \cdots, N) \tag{38}
$$

$$
m^{\beta} \ddot{\mathbf{u}}^{\beta} = \Pi^{\beta}(\mathbf{U}_I^{\alpha}, \mathbf{u}^{\gamma}) \quad (I \in P; \quad \alpha = 1, 2, \cdots, N_a; \quad \gamma = 1, 2, \cdots, N) \tag{39}
$$

where $\mathbf{U}_J^{\alpha}$ is the displacement of αth atom in the Jth node; Σ_J^{α} is the total force acting on the αth atom in the Jth node; Π^{β} is the total force acting on βth atom in the atomic region; P is the set of all nodes in the continuum region.
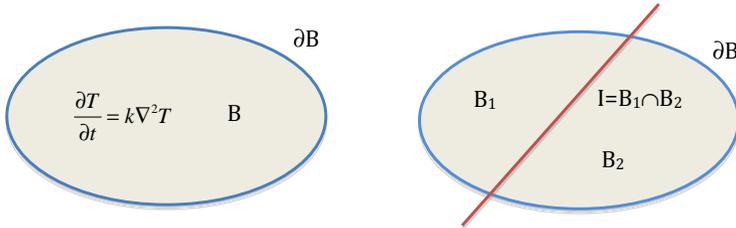

Figure 3: Schematic picture of heat conduction problem

4 Numerical Procedures

4.1 Boundary Condition at Interface

In classical heat conduction problem (cf. Fig. 3a), by virtue of Fourier's law, one has the governing equation:

$$\frac{\partial T}{\partial t} = k\nabla^2 T \tag{40}$$

where k is the heat conductivity. To secure the classical heat conduction as a well-posed problem, the following boundary conditions are imposed

$$T = T^*(\mathbf{x},t) \text{ on } \partial B_t \tag{41}$$

$$\mathbf{q} \cdot \mathbf{n} = q^*(x,t) \text{ on } \partial B_q \tag{42}$$

When the heat conduction occurs in a system composed of two homogeneous solids of different materials in perfect contact, the interface between these two homogeneous solids plays an important role in heat transfer. To ensure the compatibility and smoothness of the temperature distribution through the interface, one should have the following boundary conditions at the interface (cf. Fig. 3b)

$$T_1 = T_2$$
$$\mathbf{q}_1 \cdot \mathbf{n}_1 + \mathbf{q}_2 \cdot \mathbf{n}_2 = 0 \tag{43}$$

which means at the interface the temperature is continuous and the net heat flux is vanishing.

In this work, a more formidable interface between atomistic region and continuum region exists although these two regions are made of the same material as shown in Fig. 4. To pave the way for thermal conduction simulation in this concurrent atomistic/continuum system, a similar procedure as in classical heat conduction is adopted (cf. Fig.4)

$$T_A^* = T_e^* \equiv T^*$$
$$NT_A + \sum_{e \in E} N_e T_e = NT^* + \sum_{e \in E} N_e T^* \tag{44}$$

where T_A is the temperature in the atomic region before matching; T_e is the temperature of the eth element in the continuum region neighboring the atomic region (orange color); and E is the set of elements which are neighboring the atomic region; N_e is the total number of atoms in the eth element. From eq. (44), we have

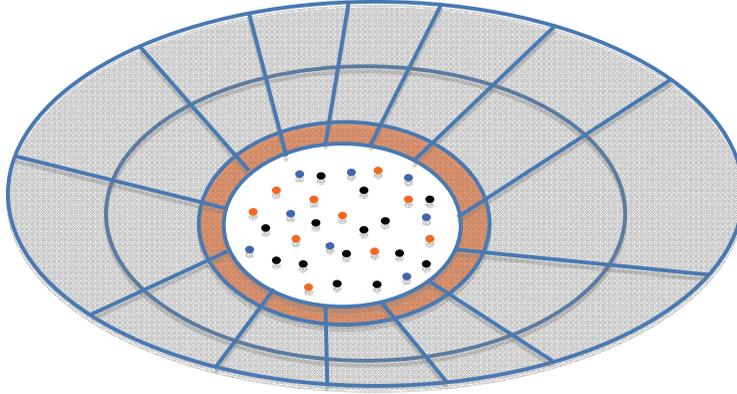$$T^* = \frac{NT_A + \sum\limits_{e \in E} N_e T_e}{N + \sum\limits_{e \in E} N_e} \tag{45}$$

Figure 4: Schematic picture of concurrent atomistic/continuum heat conduction simulation

This implies that the temperature in the atomic region and the surrounding continuum region is a calculated quantity, not a predetermined quantity, although we consider that the temperature is given as a function of space and time in the continue region.

4.2 Random velocity differences

Instantaneous values of velocity differences, $\tilde{\mathbf{u}}^i = \dot{\mathbf{u}}^i - \bar{\dot{\mathbf{u}}}$, in the atomic region are generated by sampling from a normal distribution with

$$\mu = \bar{\dot{\mathbf{u}}} = \frac{\sum\limits_{i=1}^{N} m^i \dot{\mathbf{u}}^i}{\sum\limits_{i=1}^{N} m^i} \tag{46}$$

$$\sum_{i=1}^{N} m^i (\dot{\mathbf{u}}^i - \mu) \cdot (\dot{\mathbf{u}}^i - \mu) = 3N k_B T^* \tag{47}$$

4.3 Multiple time-scale algorithms

The computational model developed in the previous section involves a two-way information exchange: the full-blown interatomic forces between two regions depend on the displacements of both regions; the fine scale atomistic simulation contributes to the temperature (cf. eq. (29)) of the atomic region; and then the coarse

scale continuum simulation provides information needed to compute the matching temperature. Different length scale corresponds to different time scale. If a single time step is adopted in both continuum and atomic regions, the stable time step depends on the Courant condition in the atomic region, i.e., $\Delta t_{cr} \leq \Delta t_A$. Therefore, computational effort will be wasted in the continuum region. If we adopt multiple time steps: larger time step Δt_C for the continuum region and smaller time step Δt_A for the atomic region, and $\Delta t_C = M\Delta t_A$ as shown in Fig. 5, the multiple time scale algorithm will offer a major advantage to improve the computational efficiency.

To solve this concurrent atomistic/continuum system with thermo-mechanical coupling, an explicit algorithm with multiple time steps, as an alternative to the temporal Green's function concept proposed by Yang and Tewary (2006), was developed based on the central difference method. Assume that accelerations, displacements and velocities are known at the nth time step. For the purpose of explanation, we denote $\mathbf{U}_I^\alpha$ as the displacement of the αth atom of the Ith node in continuum region, and $\mathbf{d}^\beta$ as the displacement of the βth atom in atomic region.

Continuum Region

$$\dot{\mathbf{U}}^\alpha_{I(n+\frac{1}{2})} = \dot{\mathbf{U}}^\alpha_{I(n)} + \frac{1}{2}\ddot{\mathbf{U}}^\alpha_{I(n)}\Delta t_C \tag{48}$$

$$\mathbf{U}^\alpha_{I(n+1)} = \mathbf{U}^\alpha_{I(n)} + \dot{\mathbf{U}}^\alpha_{I(n+\frac{1}{2})}\Delta t_C \tag{49}$$

$$T_{I(n+1)} = \begin{cases} g_I[(n+1)\Delta t_C] & I \in (P - P(E)) \\ T^*_{I(n+1)} & I \in P(E) \end{cases} \tag{50}$$

$$\ddot{\mathbf{U}}^\alpha_{I(n+1)} = (M_I^\alpha)^{-1}\mathbf{\Sigma}_I^\alpha(\mathbf{U}^\alpha_{J(n+1)}, T_{J(n+1)}, \mathbf{d}^\beta_{(n+1)}) \quad J \in P; \quad \beta = 1, 2, \cdots, N \tag{51}$$

$$\dot{\mathbf{U}}^\alpha_{I(n+1)} = \dot{\mathbf{U}}^\alpha_{I(n+\frac{1}{2})} + \frac{1}{2}\ddot{\mathbf{U}}^\alpha_{I(n+1)}\Delta t_C \tag{52}$$

where $P(E)$ is the set of all nodes associated with the elements neighboring the atomic region.

Atomic region

$$T^*_{(n)} = \frac{NT_{A(n)} + \sum\limits_{e \in E} N_e T_{e(n)}}{N_a + \sum\limits_{e \in E} N_e} \quad \Rightarrow \dot{\mathbf{d}}^\beta_{(n)} \tag{53}$$

$$\dot{\mathbf{d}}^\beta_{[n+\frac{i+1/2}{M}]} = \dot{\mathbf{d}}^\beta_{(n+\frac{i}{M})} + \frac{1}{2}\ddot{\mathbf{d}}^\beta_{(n+\frac{i}{M})}\Delta t_A \tag{54}$$

$$\mathbf{d}^{\beta}_{(n+\frac{i+1}{M})} = \mathbf{d}^{\beta}_{(n+\frac{i}{M})} + \frac{1}{2}\dot{\mathbf{d}}^{\beta}_{[n+\frac{i+1/2}{M}]}\Delta t_A \tag{55}$$

$$\ddot{\mathbf{d}}^{\beta}_{(n+\frac{i+1}{M})} = \frac{1}{m^{\beta}}\mathbf{\Pi}^{\beta}(\mathbf{U}^{\alpha}_{I(n)},\mathbf{d}^{\gamma}_{(n+\frac{i+1}{M})}) \qquad I \in P; \quad \alpha = 1,2,\cdots,N_a; \quad \gamma = 1,2,\cdots,N \tag{56}$$

$$\dot{\mathbf{d}}^{\beta}_{(n+\frac{i+1}{M})} = \dot{\mathbf{d}}^{\beta}_{[n+\frac{i+1/2}{M}]} + \frac{1}{2}\ddot{\mathbf{d}}^{\beta}_{(n+\frac{i+1}{M})}\Delta t_A \tag{57}$$

$$T^{*}_{(n+1)} = \frac{NT_{A(n+1)} + \sum\limits_{e \in E} N_e T_{e(n+1)}}{N + \sum\limits_{e \in E} N_e} \tag{58}$$

Notice that the temperature of the nodes $P(E)$ associated with the elements neighboring the atomic region E is equal to the matching temperature T^{*}.

The flow chart of the multiple time-step algorithms can be described as follows:

1. Initialize displacements, velocities, accelerations and temperatures;

2. Calculate the matching temperature T^{*} by eq.(53);

3. Randomly generate the velocity field in the atomic region $\dot{\mathbf{d}}^{\beta}$ by eqs.(46,47);

4. Update the displacements of atoms, $\mathbf{d}^{\beta}(n\Delta t_C + i\Delta t_A)$, by eqs. (54-57) at fine time step Δt_A until $t = (n+1)\Delta t_C$;

5. Repeat Step.2;

6. Update the displacements of nodes $\mathbf{U}^{\alpha}_I[(n+1)\Delta t_C]$ in continuum region by eqs.(48-52) at coarse time step Δt_C;

7. Repeat Steps. 2-6 until the end of the simulation.

5 Numerical Examples

In this section, we construct a concurrent atomistic/continuum thermo-mechanical model to study the compatibility of displacement and temperature field across the interface between atomic and continuum regions and to demonstrate a new procedure to make temperature continuous across the interface. Atomic unit are used through out this paper:

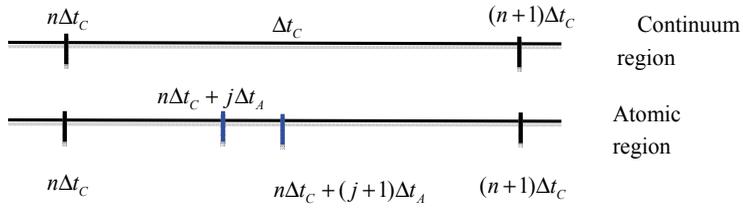Mass: $m_e = 9.10938188 \times 10^{-31}$ kilogram,

Figure 5: Arrangement of time steps in multiple-time-scale algorithm
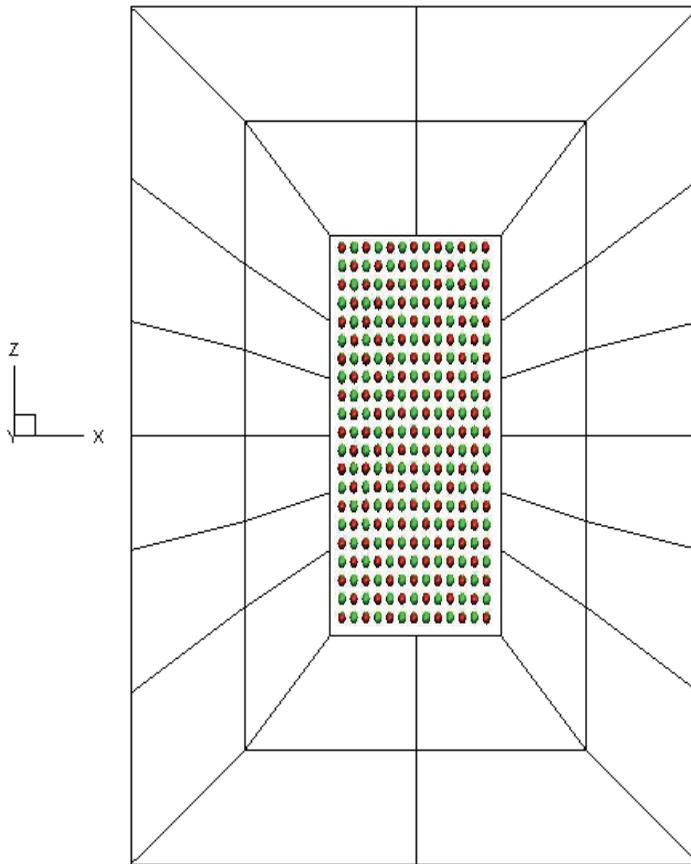

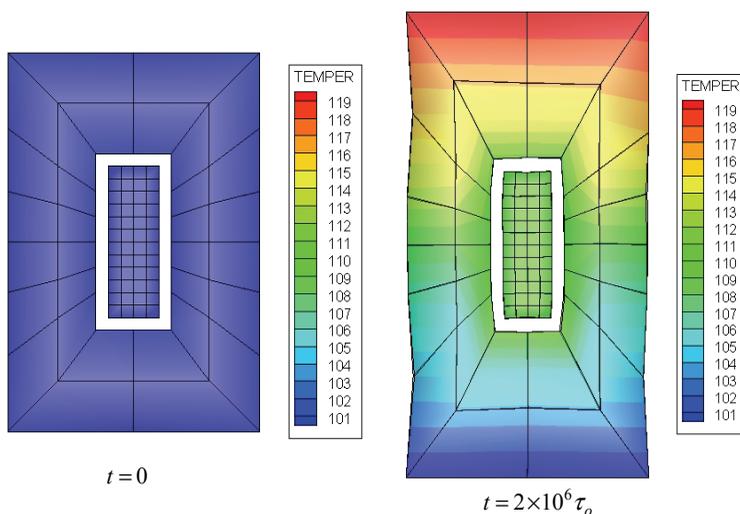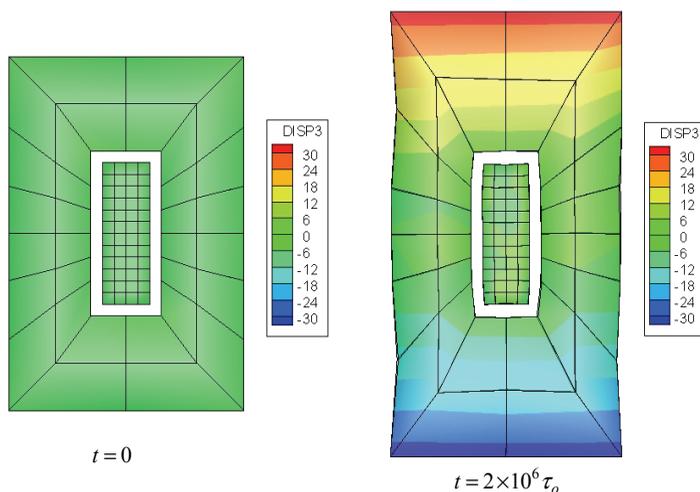Figure 6: Computational model of thermo-mechanical coupling under tensile loading

Figure 7: Temperature distribution in the specimen

Figure 8: Displacement (u_z) distribution in the specimen

Length: $a_o = 1\text{Bohr} = 0.529177249 \times 10^{-10}\text{meter}$,

Electron charge: $e = 1.602176462 \times 10^{-19}\text{Coulomb}$,

Time: $\tau_o = 2.418884326 \times 10^{-17}\text{second}$,

Energy: $E_h = 1 \text{ Hartree} = 4.3597482 \times 10^{-18}\text{Joule}$.

Here the thermo-mechanical model ($16a \times 4a \times 30a$, $a = 7.9368$ Bohr) made of Magnesium Oxide (MgO) is schematically illustrated in Fig. 6. This model consists of 2,600 atoms and 32 3-D 8-node finite elements. The boundary condition and the temperature profile in the continuum region for this model are given respectively, as follows

$$u_z^\alpha(x,y,-15a,t) = -\frac{32t}{t_T} \text{ Bohr} \quad t \le t_T$$

$$u_z^\alpha(x,y,15a,t) = \frac{32t}{t_T} \text{ Bohr} \quad t \le t_T$$

(59)

$$T(x,y,z,t) = 100 + \frac{20 \times (z+15a)}{30a} \text{ K}$$

(60)

where $t_T = 2 \times 10^6 \tau_o$ is the total time of simulation. $\Delta t_A = 5\tau_o$ and $\Delta t_C = 100\tau_o$ are used in the numerical procedures.

The Coulomb-Buckingham potentials between pairs of two atoms, $Mg - Mg$, $O - O$, $Mg - O$, are employed as

$$U^{\xi\eta} = \frac{e^\xi e^\eta}{r^{\xi\eta}} + A^{\xi\eta} e^{-r^{\xi\eta}/B^{\xi\eta}} - \frac{C^{\xi\eta}}{(r^{\xi\eta})^6}$$

(61)

where $A^{\xi\eta}$, $B^{\xi\eta}$, and $C^{\xi\eta}$ are material constants; $r^{\xi\eta} \equiv \left\| \mathbf{r}^{\xi\eta} \right\| \equiv \left\| \mathbf{r}^\xi - \mathbf{r}^\eta \right\|$. The material constants used in this work for MgO are:

$M_{Mg} = 4.57636 \times 10^4 m_e, \quad M_O = 3.01251 \times 10^4 m_e,$

$e^{Mg} = 2e, \quad e^O = -2e,$

$A^{Mg-Mg} = C^{Mg-Mg} = 0,$

$A^{Mg-O} = 47.2 \text{ Hartree}, \quad B^{Mg-O} = 0.56635 \text{ Bohr}, \quad C^{Mg-O} = 0,$

$A^{O-O} = 350.88 \text{ Hartree}, \quad B^{O-O} = 0.41415 \text{ Bohr},$

$C^{O-O} = 53.554 \text{ Hartree Bohr}^6.$

Figure 7 shows the temperature distribution of the entire specimen. It is noticed that the temperature around the interface is smooth and continuous. As expected, the temperature in the atomic region is the same as that of the neighboring elements around the atomic region. Figure 8 shows the displacement distribution of u_z in the entire specimen.

6   Summary

Atomistic field theory has been developed to circumvent the length scale problem and has its theoretical elegance in thinning redundant degrees of freedom and its computational generality in treating a wide range of grand challenging problems. In this paper we have demonstrated an approach to reconcile the compatibility between atomic region and continuum region and to calculate the temperature field of a thermo-mechanical coupling problem in a concurrent atomistic/continuum system based on the atomistic field theory. To improve the computational efficiency, we have also developed a new multiple-time-scale algorithm, which is demonstrated to behave robustly for models consisting of regions with dramatically different length scales. In the thermo-mechanical sample problem, we have shown how to calculate the matching temperature between atomic and continuum regions and how to make temperature continuous across the interface. This work enhances the understanding of some fundamental characteristics of the thermo-mechanical coupling problem in the concurrent atomistic/continuum system.

Reference

Abraham, F.F.; Broughton, J.Q.; Bernstein, N.; Kaxiras, E. (1998): Spanning the continuum to quantum length scales in a dynamic simulation of brittle fracture. *Europhys. Lett.*, 44, pp.783-787.

Belytschko, T.; Xiao, S. P. (2003): Coupling methods for continuum model with molecular model. *J. Mult. Comput. Engrg.*, 1, pp.115-126.

Chen, Y. (2006): Local stress and heat flux in atomistic systems involving three-body forces. *Journal of Chemical Physics*, 124, pp.054113.

Chen, Y. (2009): Reformulation of microscopic balance equations for multiscale materials modeling. *J. Chem. Phys*, 130(13), pp.134706-134706-6.

Chen, Y.; Lee, J.D. (2005): Atomistic formulation of a multiscale theory for nano/micro physics. *Philosophical Magazine*, 85, pp.4095-4126.

Cheung, K.S.; Yip, S. (1991): Atomic-level stress in an inhomogeneous system. *J. Appl. Phys.*, 70(10), pp.5688.

Dove, M. (1993): Introduction to Lattice Dynamics, Cambridge University Press, Cambridge.

Fish, J.; Nuggehally, M.A.; Shephard, M.S.; Picu, C.R.; Badia, S.; Parks, M.L.; Gunzburger, M. (2007): Concurrent AtC coupling based on a blend of the continuum stress and the atomistic force. *Computer Methods in Applied Mechanics and Engineering*, 196(45-48), pp.4548–4560.

Haile, J.M. (2001): Molecular dynamics simulation: elementary methods, Wiley-

Interscience, New York.

Hardy, R.J. (1982): Formulas for determining local properties in molecular-dynamics simulations: Shock waves. *J. Chem. Phys.* 761), pp. 622.

Kadowaki, H.; Liu, W.K. (2005): A multiscale approach for the micropolar continuum model, *CMES: Computer Modeling in Engineering and Science* vol.7, 269-282

Knap, J.; Ortiz, M. (2001): An analysis of the quasicontinuum method. *J. Mech. Phys. Sol.,* 49, pp.1899–1923.

Lee, J. D.; Wang, X.Q.; Chen, Y. (2009a): Multiscale computational for naon/micromaterial. *Journal of Engineering Mechanics*, 135, pp.192-202.

Lee, J. D.; Wang, X.Q.; Chen, Y. (2009b): Multiscale material modeling and its application to a dynamic crack propagation problem. *Theoretical and Applied Fracture Mechanics*, 51, pp.33-40.

Ma, J.; Lu, H.; Wang, B.; Hornung, R.; Wissink, A.; Komanduri, R. (2006): Multiscale Simulation Using Generalized Interpolation Material Point (GIMP) Method and Molecular Dynamics (MD), *CMES: Computer Modeling in Engineering & Sciences*, vol. 14 (2), 101-118

Marian, J.; Venturini, G.; Hansen, B.L.; Knap, J.; Ortiz, M.; Campbell, G.H. (2010): Finite-temperature extension of the quasicontinuum method using Langevin dynamics: entropy losses and analysis of errors. *Modelling Simul. Mater. Sci. Eng.*, 18, pp.015003.

Parks, M.L.; Bochev, P.B.; Lehoucq, R.B. (2008): Connecting atomistic-to-continuum coupling and domain decomposition. *Multiscale Modeling & Simulation*, 7(1), pp.362–380.

Raghavan, P.; Ghosh, S. (2004): Adaptive multiscale computational modeling of composite materials, *CMES: Computer Modeling in Engineering and Science* vol.5, 151-170

Rudd, R.E.; Broughton, J.Q. (2001): Concurrent coupling of length scales in solid state systems. *Phys. Status Solidi B*, 217, pp.251-291.

Shen, S.; Atluri, S.N. (2004a): Multiscale simulation based on the meshless local Petrov-Galerkin (MLPG) method, *CMES: Computer Modeling in Engineering & Sciences* 5 vol. (3), 235-255

Shen, S.; Atluri, S.N. (2004b): Computational nano-mechanics and multi-scale simulation, *CMC: Computers, Materials & Continua* 1vol. (1), 59-90

Shen, S.; Atluri, S.N. (2004c): Atomic-level stress calculation and continuum-molecular system equivalence , *CMES: Computer Modeling in Engineering & Sciences* vol. 6 (1), 91-104

Shenoy, V.; Shenoy, V.; Phillips, R. (1999): Finite temperature quasicontinuum method. *Mater. Res. Soc. Symp. Proc*, 538, pp.465-471.

Smith, G.S.; Tadmor, E. B.; Bernstein, N.; Kaxiras, E. (2001): Multiscale simulations of silicon nanoindentation. *Acta Mater.,* 49, pp.4089-4101.

Steinmann, P.; Elizondo, A.; Sunyk, R. (2006): Studies of validity of the Cauchy-Born rule by direct comparison of continuum and atomistic modeling. *Modelling Simul. Mater. Sci. Eng.*, 15, pp. 271-281.

Tadmor, E. B.; Ortiz, M.; Phillips, R. (1996): Quasicontinuum analysis of defects in solids. *Philo. Mag.*, 73, pp.1529-1563.

Tadmor, E. B.; Smith, G.S.; Bernstein, N.; Kaxiras, E. (1999): Mixed finite element and atomistic formulation for complex crystals. *Physical Review B,* 59, pp.235-245.

Wagner, G.J.; Liu, W.K. (2003): Coupling of atomistic and continuum simulations using a bridging scale decomposition. *J. Comput. Phys.*, 190, pp.249–274.

Xiao, S. P.; Belytschko, T. (2004): A bridging domain method for coupling continua with molecular dynamics. *Comput. Methods Appl. Mech. Engrg.*, 193, pp.1645-1669.

Xiao, S.P.; Yang, W.X. (2007): A temperature-related homogenization technique and its implementation in the meshfree particle method for nanoscale simulations, *Int. J. Numer. Meth. Engng*, 69, pp.2099-2125.

Yang, B.; Tewary, V.K.(2006): Efficient Green's function modeling of line and surface defects in multilayered anisotropic elastic and piezoelectric materials, *CMES: Computer Modeling in Engineering and Science* vol.15, 165-177.